NEANDC (OR) - 152 "L"
Part B
INDC (SWT) - 13 / L

PROGRESS REPORT TO NEANDC FROM SWITZERLAND

June 1979

F. Widder

Swiss Federal Institute for Reactor Research
Würenlingen

~~NOT FOR PUBLICATION~~

PREFACE

This document contains information of a preliminary or private nature and must be used with discretion. Its contents may not be quoted, abstracted, reproduced, transmitted to libraries or societies or formally referred to without the explicit permission of the originator.

CONTENTS

I. Institut de Physique, Université de Neuchâtel

(Dir.: Prof. Jean Rossel)

1. n-d elastic differential cross section at 2.48 and 3.28 MeV

P. Chatelain, Y. Onel[+] and J. Weber

The final results have been published {1}. They show cross section values at large scattering angles ($-0.8 > \cos\theta_{cm} > -1.0$) that are larger than earlier measurements {2}. The agreement with Alt's calculations {3} is good at 3.28 MeV. At 2.48 MeV these calculations (as well as the calculations of other authors) lay below our data at large angles and also below Seagrave's data {2} at small angles.

In a near future we shall start measurements of the n-d elastic scattering cross section at 2.0 and 3.0 MeV with the purpose in praticular of making precise comparison between p-d {4} and n-d scattering at these two energies.

References

{1} P. Chatelain, Y. Onel and J. Weber, Nucl. Phys. A319 (1979) 71 and Nucl. Instr. Meth. 151 (1978) 519.

{2} M.D. Goldberg, V.M. May and J.R. Stehn, Brookhaven Nat. Lab. Report BNL-400, vol. 1 (1962).

{3} E.O. Alt and B.L.G. Bakker, Z. Physik, A273 (1975) 37.

{4} D.C. Kocher and T.B. Clegg, Nucl. Phys. A132 (1969) 455.

2. Depolarisation factor $D(\theta)$ for the $d(\vec{n},\vec{n})d$ reaction at 2.45 MeV

D. Bovet, P. Chatelain, Y. Onel[+] and J. Weber

+ Present address: Université de Genève, Département de physique nucléaire et corpusculaire, 1211 Genève 4

The measurements of $D(\theta)$ has been completed. The results have been or will be published {1}. They are listed in Table 1.

θ_L	θ_{CM}	$D(\theta)$
20	29.8	0.21 ± 0.09
30*	44.5	0.31 ± 0.15
40.5*	59.5	0.34 ± 0.17
55*	79.2	0.54 ± 0.17
62	88.2	0.53 ± 0.17
70*	98.0	0.69 ± 0.15
80	109.5	0.53 ± 0.11
90	120.0	0.55 ± 0.11

Table 1: Our results of $D(\theta)$. *: already published by D. Bovet et al.{1}. The quoted standard deviations are essentially statistical.

References

{1} D. Bovet, P. Chatelain, R. Viennet and J. Weber, J. Phys. G 4 (1978) 1313.

P. Chatelain, Université de Neuchâtel, Thesis.

3. Phase shift analysis of the (n,d) and elastic scattering

P. Chatelain, R. Viennet and J. Weber

Our cross section and $D(\theta)$ data (among others) have been used as input data to phase shift analyses. Preliminary results confirm the fact that partial waves up to $\ell = 3$ and $\ell = 5$ are necessary (at 2.45 MeV and 3.27 MeV resp.) to explain the cross section data and that even higher partial waves ($\ell = 4$) have to be included to explain the $D(\theta)$ data. Moreover it

has been verified that doublet phases have a large influence in fitting the $D(\theta)$ data.

In the future our ERA code {1} will be modified to include partial waves higher than $\ell = 2$ and our $D(\theta)$ data. It is indeed felt that this procedure should give more reliable results than the usual phase shift analysis procedure.

References

{1} D. Bovet, P. Chatelain, R. Viennet and J. Weber, J. Phys. G 4 (1978) 1313.

II. Institut de Physique, Université de Fribourg

(Dir.: Prof. Dr. O. Huber)

Nuclear levels in ^{238}Np*

V.A. Ionescu, Jean Kern, R.F. Casten†, W.R. Kane††, I. Ahmad††, J. Erskine††, A.M. Friedman †† and K. Katori††

In the last twelve years the level schemes of a number of doubly odd nuclei in the rare earth deformed region have been successfully investigated. Due to the high nuclear level density, it has been necessary, in general, to combine the results of several precision experiments. From these studies it has been recently possible to draw important conclusions regarding the residual proton-neutron interaction {1}.

Very little attention has been given until now to the spectroscopy of the odd-odd nuclei in the actinide region. Several circumstances are responsible for this situation: The level density is expected to be still higher; investigations using the (n,γ) reaction are hampered by the radioactivities of the target and of the final nucleus; large neutron fission cross sections for the target or the final nucleus may further increase the difficulty: finally, only limited data on the adjacent odd neighbours had been obtained by reaction spectroscopy, so that the experimentalists were deterred from studying the more difficult doubly odd nuclei by such methods. The latter argument has become less significant in the last decade, since detailed studies using direct transfer reactions have significantly improved our konwledge of the level structure of many odd-A nuclei in this region of the nuclear chart, making attractive an attempt to study odd-odd actinide nuclei by reaction spectroscopy.

* Work supported in part by the Swiss National Science Foundation

† Physics Department, Brookhaven National Laboratory, Upton, NY 11973, USA

†† Physics Division, Argonne National Laboratory, Argonne, Illinois 60 439, USA

The choice of a suitable nucleus is relatively limited. The selection of ^{238}Np was made because ^{237}Np has a long half-life (2.2×10^6 y), is commercially available and can thus be used as a target in the (n,γ) and (d,p) reactions. In addition useful information was already available on the level scheme of ^{238}Np. The ground state spin, determined by the atomic beam magnetic resonance method, has been found {2} to be 2. Asaro et al. {3,4} studied the α-decay of ^{242m}Am. They observed seven α-groups and seventeen γ-ray transitions. From these results the existence of fifteen excited states could be more or less reliably established. Their energies are given, for comparison, together with our results in table 5.

In the following tables the main results of experiments performed at three laboratories are given: High and low energy thermal neutron capture γ-rays have been observed by the Fribourg group with a pair and an anti-Compton spectrometer, and also with single Ge(Li) diodes {5}; primary transitions from resonance capture have been studied in Brookhaven, while proton groups from the ^{237}Np (d,p) reaction were analysed in Argonne with a magnetic spectrograph. A more detailed description is given in {6} and a summary of the results has been reported in a symposium {7}.

TABLE 1

High energy capture γ-ray transitions from the $^{237}Np(n, \gamma)$ reaction and the levels of ^{238}Np

E (keV)	ΔE (keV)	I_{rel} [a])	ΔI_{rel} [a])	E_{exc} [c]) (keV)	ΔE_{exc} [b]) (keV)
5487.6	0.6	5.7	0.9	0.4	0.6
5352.0	0.15	100	4	136.0	0.3
5305.7	0.6	8	1.6	182.3	0.6
5297.4 [d])	0.6	5	1.5	190.6	0.6
5271.5 [e])	1.0	6	2	216.5	1
5238.05	0.15	35.6	2.3	250.0	0.3
5229.3 [f])	0.5	7.5	1.5	258.7	0.5
5153.7 [f])	0.8	4.2	1.5	334.3	0.8
5140.5	0.4	11.5	1.9	347.5	0.4
5120.0	0.5	21	3	368.0	0.5
5115.2	0.6	14	3	372.8	0.6
5101.6	0.3	16	2	386.4	0.4
5046.3	0.2	39	3	441.7	0.3
5030.55	0.15	56.6	3.2	457.4	0.3
4960.0	0.6	9	2	528.0	0.6
4920.4 [g])	0.5	8	2	567.6	0.5
4903.8 [h])	0.3	18.5	3	584.2	0.4
4886.5	0.7	9	2	601.5	0.7
4868.5	0.2	32.4	2.5	619.5	0.3
4841.0 [f])	0.7	7	2	647.0	0.7
4814.4	0.2	33.5	2.3	673.7	0.3
4795.5	0.5	5	1.5	692.6	0.5
4778.80	0.15	54	3	709.2	0.3
4765.6	0.7	10	2	722.4	0.7
4723.9	0.6	7.4	1.9	764.3	0.6
4705.6	0.5	9	2	782.4	0.5
4690.7 [h])	0.3	16	6	797.3	0.4
4687.7	0.8	15	6	800.4	0.8
4678.3	0.2	42.5	4	809.8	0.3
4674.2	0.7	11	3	813.9	0.7
4653.4	0.5	11	2	834.7	0.5
4619.1 [g])	0.4	19	2	869.0	0.4
4584.8	0.3	21	2	903.3	0.4
4571.5	0.8	9	2	916.6	0.8
4559.0 [f])	0.6	8	2	929.1	0.6
4539.2 [f])	0.5	12.3	2.7	948.9	0.5
4517.4 [f])	0.6	7	2	970.7	0.6
4501.6 [f])	0.3	20.3	2.4	986.5	0.4
4461.5 [f])	0.6	8	2	1026.6	0.6
4454.7 [f])	0.7	7	2	1033.4	0.7

TABLE 1 (continued)

E (keV)	ΔE (keV)	I_{rel} [a])	ΔI_{rel} [a])	E_{exc} [c]) (keV)	ΔE_{exc} [b]) (keV)
4441.6 [f])	0.6	6.9	2	1046.5	0.6
4422.9 [f])	0.4	11	2	1065.2	0.4
4407.1 [f])	0.6	6	2	1081.0	0.6
4399.1 [f])	0.6	8	2	1089.0	0.6
4380.3 [g])	0.7	17	3	1107.8	0.7
4368.5 [f])	0.7	10	3	1197.6	0.7
4345.1	0.5	11	3	1143.0	0.5
4325.0	0.4	27	3	1153.1	0.4
4312.0	0.5	10.4	2.4	1176.0	0.5
4232.0	0.2	48	3	1256.1	0.1
4227.6	0.6	13	3	1260.5	0.6
4212.0	0.4	16	3	1276.1	0.4
4196.8	0.3	17	3	1291.3	0.4
4174.6	0.2	24	3	1313.5	0.3
4157.4	0.5	28	3	1330.7	0.5
4123.3	0.7	15.3	3.5	1364.8	0.7
4118.3	0.7	13.4	3.4	1369.8	0.7
4112.5	0.3	19.5	3.5	1375.6	0.4
4103.5	0.2	30	4	1384.6	0.3
4095.3	0.4	13	3	1392.8	0.4
4079.6	0.5	16.6	3.3	1408.5	0.5
4042.4	0.6	11.5	3	1445.7	0.6
4004.0 [g])	0.8	13	3	1484.1	0.8
3995.3 [f])	0.7	8	3	1492.8	0.7
3979.1	0.4	13	3	1509.0	0.4
3941.6	0.7	14	3	1546.5	0.7
3776.6	0.4	20	4	1711.5	0.4
3665.6	0.5	13	4	1822.5	0.5
3383.8	0.5	16	4	2104.3	0.5
3378.6	0.4	19	5	2109.5	0.4
2630.7	0.6	22	7	2857.4	0.6

[a]) It is estimated that the scale unit corresponds to one photon/10^4 capture.
[b]) Relative errors only.
[c]) Assuming $Q = 5488.1 \pm 0.2$ keV.
[d]) Probable ^{15}N impurity.
[e]) Doublet. One component is from ^{15}N.
[f]) Doubtful.
[g]) Possible background contribution.
[h]) An Al background contribution has been subtracted.

TABLE 2

Low energy transitions from the $^{237}Np(n, \gamma)$ reaction

E (keV)	ΔE	I_{rel}	ΔI	Assignment
49.37	0.03	48	11	136.0– 86.6
53.60 [a])	0.12	1	0.3	
57.95 [a])	0.15	1	0.3	
59.2	0.2	0.9	0.3	121.8– 62.2
60.16	0.04	3.5	0.9	86.6– 26.4
72.89	0.03	4.2	0.8	
73.81	0.04	3.1	0.6	136.0– 62.2
79.78	0.08	0.8	0.2	
82.23	0.03	4.1	0.7	
102.64 [a])	0.12	3.2	0.7	
105.95 [a])	0.25	0.8	0.4	
107.21	0.05	4.8	0.5	
109.69	0.04	9.9	0.6	136.0– 26.4
115.76 [a])	0.09	2.4	0.4	
121.79	0.04	1.5	0.1	121.8– 0
124.3	0.2	0.3	0.1	368.4–243.9
126.40	0.13	0.5	0.1	
136.000	0.025	4.2	0.2	136.0– 0
144.45	0.08	0.8	0.1	
152.94	0.04	4.0	0.3	368.4–215.5
153.74	0.06	2.9	0.3	
156.43	0.03	34	2	182.8– 26.4
160.63	0.04	2.9	0.2	
176.53	0.07	1.1	0.2	
182.85	0.03	100	7	182.8– 0
189.08	0.04	3.4	0.3	215.5– 26.4
215.49	0.04	5.6	0.4	215.5– 0
217.60	0.09	2.2	0.4	243.9– 26.4
218.5	0.2	0.7	0.3	
232.37	0.04	4.5	0.4	368.4–136.0
233.64	0.08	1.5	0.2	
236.00	0.04	5.1	0.4	
243.92	0.03	27	2	243.9– 0
250.30	0.05	2.5	0.2	
264.70	0.13	0.9	0.2	
281.80	0.15	0.8	0.2	368.4– 86.6
289.0	0.2	1.0	0.3	
294.1	0.2	1.4	0.5	
297.70 [a, b])	0.15	6	2	
332.15	0.04	6.9	0.6	

TABLE 2 (continued)

E (keV)	ΔE	I_{rel}	ΔI	Assignment
391.25 [a, b])	0.10	1.3	0.3	
405.20	0.15	1.7	0.3	
430.85	0.06	4.7	0.4	
461.55 [a])	0.15	2.3	0.5	
496.61 [a])	0.09	3.9	0.5	
530.7	0.2	1.8	0.4	
538.30	0.12	2.6	0.4	
541.20	0.12	2.8	0.4	
551.65 [b])	0.12	1.4	0.5	
555.25	0.15	2.3	0.4	
557.20	0.15	2.8	0.4	
584.35	0.15	3.0	0.6	646.6– 62.2
606.7	0.3	2.4	0.7	
620.10	0.15	3.8	0.6	646.6– 26.4
646.8	0.2	4.2	0.8	646.6– 0
648.2	0.2	3.7	0.8	

[a]) Doubtful.
[b]) Possible background contribution.

TABLE 3

Results of the $^{237}Np(n, \gamma)^{238}Np$ reaction at thermal and resonant neutron energies [a])

Weighted av. energies				Thermal		0.489 eV		1.33 eV		1.48 eV $J^{\pi}_{capt} = 2^+$		5.8 eV $J^{\pi}_{capt} = 3^+$	
E_γ (keV)	E_{ex} (keV)	J	π [b])	E_γ (keV)	I_γ (rel)	E_γ (keV)	I_γ (rel)	E_γ (keV)	I_γ (rel)	E_γ (keV)	I_γ (rel)	E_γ (keV)	I_γ (rel)
5352.2(0.3)	136.0	1–3	–	5352.1(0.3)	100 (10)					5352.6(1.8)	7.9(2.9)		
5308.4(1.5) [g])	179.8(1.0)	2, 3	–			5308.3(1.2)	10 (2)	5310.2(1.8)	19 (6)	5307.7(1.2)	51 (9)	5310.2(3.0)	34(15)
[5304.4(2.0)]	[183.8(2.0)]	2–4	±					[5302.9(1.8)]	[10 (6)]			[5305.9(3.0)]	[16 (8)]
5272.9(1.0)	215.3(1.0)	2, 3	–	5269.0(3.0)	5.4(2.4)	5272.5(0.3)	89 (9)	5271.2(2.0)	23 (9)	5274.2(1.0)	57 (9)	5273.9(3.0)	32 (8)
5241.7(1.5) [g])	246.5(1.5)	1–3	±	5242.9(3.0)						5241.2(1.6)	22 (6)		
5238.6(1.0)	249.6(1.0)	1–4	±	5238.6(3.0)	33 (10) [c])			5238.6(1.0)	19 (8)				
5232.0(1.5)	256.2(1.5)	1–3	±	5234.3(3.0)		5233.4(2.3)	35(14)	5230.7(1.5)	22 (8)	5234.6(1.5)	15 (6)		
5202.2(1.0)	286.0(1.0)	1–4	±	5202.2(1.0)	2.8(1.2)								
5166.8(1.8)	321.4(1.8)	1–3	±	[d])						5166.8(1.8)	28 (9)		
5155.7(0.8)	332.5(0.8)	1–3	±	[d])						5155.7(0.8)	68 (12)		
5138.2(1.0)	350.1(0.8)	1–3	–	[e])		[e])		5139.6(1.2)	74(20)	5137.5(0.8)	37 (15)		
5120.0(1.0)	368.2(1.0)	1–3	±	5120.8(1.0)	10 (3)					5118.5(1.8)	49 (12)		
5114.1(0.9)	374.1(0.9)	1–4	–			5114.8(0.6)	89 (9)	5112.8(1.0)	32(10)				
5102.4(0.6)	385.8(0.6)	1–4	±	5103.0(1.5)	10 (4)	5101.8(0.4)	40 (6)						
5047.8(1.5)	440.4(1.5)	1–4	±	5047.2(1.5)	37 (9)	5048.4(1.5) [f])	30 (7)						
5031.5(0.6)	456.7(0.6)	1–4	–	5031.3(0.5)	70 (7)			5032.7(1.2)	68(10)				
4961.0(0.7)	527.2(0.7)	1–3	–			4960.0(1.0)	100(10)			4961.8(0.5)	100 (10)		
4921.9(0.7)	566.3(0.7)	1–3	–			4922.4(1.0)	52 (9)	4921.4(0.4)	100(20)	4924.5(3.0)	25 (9)		
4888.2(1.5)	600.0(1.6)	1–4	±			4890.0(2.3)	16 (6)	4887.0(1.2)	31(10)				
4864.4(1.5)	623.8(1.5)	1–4	±	[e])		4864.4(1.5)	27 (7)						
4842.0(1.3)	646.2(1.3)	1–3	±	[e])		4840.6(1.0)	53 (9)	4844.2(1.3)	29(10)	4843.0(2.0)	21 (10) [h])		
4813.9(0.8)	674.3(0.8)	1–3	–	4813.6(0.3)	37 (3.7)	4813.3(2.0)	39(18)	4813.1(1.5)	15 (6)	4815.8(0.8)	86 (9)		
4795.7(0.6)	692.5(0.6)	2, 3	–	[e])				4795.0(1.5)	15 (8)	4796.1(0.6)	52 (12) [h])	4793.7(3.0)	100(10)

[a]) Transition energies in the first column are a weighted average over thermal and resonant data. Excitation energies are deduced assuming an energy of 136.0 keV for the state populated by the 5352.2 keV transition. In addition to the relative energy uncertainties indicated in keV in parentheses there is an uncertainty of ±1.0 keV in the overall absolute energy scale. The uncertainties in intensities are in the same units as the intensities themselves. The strongest transition for each neutron energy is given an intensity of 100.

[b]) The J^{π} values are deduced assuming dipole primary transitions and assigning E1 multipolarity to the few strongest transitions. In addition, a level populated at least moderately strongly at two or more neutron energies is assigned negative parity. Where the parity ± is shown, it indicates that, though negative parity is still more likely, positive parity cannot be safely ruled out. The parity assignments assume single levels. If the 374 keV level is a doublet (see text) the parity of each member can be either + or – based on the resonance capture data.

[c]) Partially resolved multiplet, summed intensity given.

[d]) Weak peak definitely present in spectrum: no reliable intensity can be extracted.

[e]) Peak obscured by contaminant line or first escape peak.

[f]) Possible doublet.

[g]) Complex group at most neutron energies, most likely decomposition given.

[h]) Peak contains contribution, form first escape peak of higher energy γ-ray, which has been subtracted to obtain the listed intensity.

TABLE 4

Excitation energies of levels in ^{238}Np, differential cross sections in (d,p), and orbital assignments

Excitation energy (keV)	$d\sigma/d\Omega$ 85° (μb/sr)	$d\sigma/d\Omega$ 135° (μb/sr)	$R = \frac{d\sigma(85^\circ)}{d\sigma(135^\circ)}$	Assignment [a] I^π	Assignment [a] orbitals
0	26.4±1.1	19.7±1.4	1.3	2^+	A-C
26.5±0.8	17.6±1.0	16.2±1.3	1.1	3^+	A-C
62.0±0.7	6.9±1.1	12.5±1.5	0.55	4^+	A-C
86.9±0.5	29.2±2	28.6±2.2	1.0	3^+	A+C
107.3±1.2	4.2±1	8.9±1.4	0.47	5^+	A-C
123.0±0.5	13.9±1.5	15.9±1.8	0.87	4^+	A+C
165.1±1.2	10.0±1.3	13.5±1.5	0.74	5^+	A+C
221.2±0.8	8.6±1.2	9.7±1.0	0.88	6^+	A+C
278.1±1.0	15.5±1.5	23.6±4.1	0.66	5^+	A+D
328.6±0.5	14.2±2.0	23.8±4.1	0.60	6^+	A+D
374.7±1.0	11.0±1.6	18.9±2.6	0.58	2^+, 3^+	A-D
389.9±0.9	13.8±1.7	23.6±2.8	0.58	7^+	A+D
409.5±0.5	2.9±1.0	8.5±1.8	0.34		
431.3±0.6	8.2±1.3	15.4±2.3	0.54	4^+	A-D
456.3±0.7	8.4±1.4	14.0±2.2	0.60	5^+	A-D
524.2±0.6	7.6±2.0	7.3±1.6	1.0	6^+	A-D
603.7±0.6	3.3±1.0	5.6±1.0	0.59		
630.6±1.3	6.2±1.2	10.0±1.3	0.62		
648.7±0.5	5.9±1.2	4.7±1.0	1.2		
675.6±0.5	4.7±1.1	7.1±1.2	0.66		
691.9±0.6	9.7±1.5	15.6±1.6	0.62		

[a]) $A = \frac{5}{2}^+ [642]$, $B = \frac{5}{2}^- [523]$, $C = \frac{1}{2}^+ [631]$, $D = \frac{5}{2}^+ [622]$.

TABLE 5

Energies and assignments of the levels observed in the different experiments

^{242m}Am α-decay	High energy (n, γ)	Low energy (n, γ)	Resonance capture	(d, p)	$I^{\pi}K$	Q [a])	Configuration [b])
0.0	0.4±0.6	0.0		0	2^+2	A	**A−C**
26.4		26.39±0.03		26.5±0.8	3^+2	A	A−C
62.7		62.22±0.05		62.0±0.7	4^+2	A	A−C
86.7		86.61±0.03		86.9±0.5	3^+3	A	**A+C**
106.1				107.3±1.2	5^+2	A	A−C
121.8		121.78±0.04		123.0±0.5	4^+3	A	A+C
136.0	136.0±0.3	136.01±0.02	136.0 [c])		3^-3	A	**B+C**
165.9				165.1±1.2	5^+3	A	A+C
179.2			179.8±1.0		4^-3	A	B+C
[d])	182.3±0.6	182.83±0.03	183.8±2.0		2^-2	A	**B−C**
	216.5±1.0	215.48±0.03	215.3±1.0		3^-2	A	B−C
				221.2±0.8	6^+3	A	A+C
233.1					5^-3	A	B+C
		243.93±0.03	246.5±1.5				
	250.0±0.3		249.6±1.0				
	258.7 [e])±0.5		256.2±1.5		4^-2	B	B−C
275.7				278.1±1.0	5^+5	B	**A+D**
			286.0±1.0		1^-0	C	**B−D**
301.0					6^-6	B	**A+E**
			321.4±1.8				
				328.6±0.5	6^+5	B	A+D
	334.3 [e])±0.8		332.5±0.8		1^+0	C	**A−D**
342.6					5^-5	A	**B+D**
	347.5±0.4		350.1±0.8		3^-0	B	B−D
	368.0±0.5	368.2 ±0.04	368.2±1.0		2^-0	B	B−D
	372.8±0.6		374.1±0.9	374.7±1.0	2^+0	B	A−D
					3^+0	C	A−D
	386.4±0.4		385.8±0.6				
				389.9±0.9	7^+5	B	A+D
410				409.5 [g])±0.5	6^-5	B	B+D
				431.3±0.6	4^+0	B	A−D
	441.7±0.4		440.4±1.5		4^-0	B	B−D
				456.3±0.7	5^+0	C	A−D
	457.4±0.3		456.7±0.6				
465							
486							
				524.2±0.6	6^+0	B	A−D
	528.0±0.6		527.2±0.7				
	567.6 [f])±0.5		566.3±0.7				
	584.2±0.4						
	601.5±0.7		600.0±1.6				
				603.7±0.6			
	619.5±0.3		623.8±1.5				
				630.6±1.3			
	647.0 [e])±0.7	646.58±0.1	646.2±1.3	648.7±0.5			
	673.7±0.3		674.3±0.8	675.6±0.5			
	692.6±0.5		692.5±0.6	691.9±0.6			

The data for the ^{242m}Am decay are from ref. [4]).

[a]) Q indicates the reliability of the assignment: A = reliable; B = probable; C = possible.

[b]) A = $\pi\frac{5}{2}^+[642\uparrow]$; B = $\pi\frac{5}{2}^-[523\downarrow]$; C = $\nu\frac{1}{2}^+[631\downarrow]$; D = $\nu\frac{5}{2}^+[622\uparrow]$; E = $\nu\frac{7}{2}^+[624\downarrow]$. Band-heads are written in bold characters.

[c]) Adopted energy to determine the reaction Q-value.

[d]) This level has been disclosed in a new investigation by Hoff.

[e]) Level feeded by a doubtful transition. [f]) Possible background contribution in the feeding transition.

[g]) It is not clear if this level is the same as that observed in α-decay. The assignment is valid for the latter.

A comparison of the experimental and calculated (d,p) cross sections displays a qualitative agreement. The experimental values are however significantly larger than predicted for the high spin states. This problem was already noted in the study of odd-A nuclei and tentatively explained by an inadequate treatment of the asymptotic tail of the bound state wave function in the DWBA calculation {8}. Differences may have various other origins such as incorrect optical model parameters, which influence the values of $\Phi_l(\Theta)$, inaccurate C_{jl} Nilsson expansion coefficients, improper occupation probabilities U_ν^2, or neglected Coriolis interactions. A more detailed analysis does not seem useful until more data are available and the assignments of several levels more certain. A new investigation of the ^{242m}Am α-decay is presently being performed in Livermore {9} while new (n,e^-) and (n,γ) experiments, using the spectrometers BILL and GAMS at ILL/Grenoble, are under way.

In conlusion we note that all rotational bands built on the intrinsic configurations that we have labelled A, B, D and D are now more or less reliably established (see table 5). Four Gallagher-Moszkowski splittings and two Newby terms are thus now available in ^{238}Np for the determination of residual interactions in the actinide region.

References

{1} J.P. Boisson, R. Piepenbring and W. Ogle, Phys. Reports 26C (1976) 99

{2} R.G. Albridge, J.C. Hubbs and R. Marrus, Phys. Rev. 111 (1958) 1157

{3} F. Asaro, M.C. Michel, S.G. Thompson and I. Perlman, Proc. Rutherford Jubilee Int. Conf., Manchester 1961, ed. J.B. Birks (Heywood, London 1961) p. 311

{4} F. Asaro, M.C. Michel, S.G. Thompson and I. Perlman, private communication quoted by C.M. Lederer, J.M. Hollander and I. Perlman, Table of isotopes (Wiley, NY, 1969);

E. Browne and F. Asaro, private communication quoted by Y.A. Ellis, Nucl. Data Sheets B4 (1970) 635

{5} V.A. Ionescu and J. Kern, Report of the University of Fribourg IPF-SP-005 (1975)

{6} V.A. Ionescu, Jean Kern, R.F. Casten, W.R. Kane, I. Ahmad, J. Erskine, A.M. Friedman and K. Katori, Nucl. Phys. A313 (1979) 283

{7} J. Kern, V.A. Ionescu, R.F. Casten, W.R. Kane, I. Ahmad, J. Erskine, A.M. Friedman and K Katori, 3rd Int. Symp. on neutron capture gamma-ray spectroscopy, Brookhaven 1978, contr. no. 41

{8} J.R. Erskine, Phys. Rev. C5 (1972) 959

{9} R.W. Hoff, Livermore, private communication

III. Physik-Institut der Universität Zürich

(Dir.: Prof. E. Brun)

^{6}Li+α - scattering from 1.4 to 3.0 MeV

P. Heusi, R. Pixley, V. Meyer

The scattering of α-particles on ^{6}Li has been studied between 1.4 and 3 MeV laboratory energy. In order to fit the resonances leading to the compound nucleus ^{10}B which occur in this energy range it is necessary to have a good phase shift description of the background cross section. Our aim was to understand this background which shows a pronounced rise towards back angles in terms of an exchange mechanism. For that purpose angular distributions were measured at six energies between the narrow resonances with special attention to an absolute calibration. Since the absolute cross sections on Li-targets given in the literature are often unreliable due to the chemical instability of Li we present here the results of these measurements. A theoretical treatment of the data including contributions from Coulomb- and exchange scattering as well as from a broad $\ell = 0$ - resonance at $E_{lab} = 1.2$ MeV will be published elsewhere.

The He^{+}-beam accelerated by the Van de Graaff-accelerator of the Physik-Institut of the University of Zürich was scattered by a target consisting of a self-supporting carbon foil onto which appr. 3 μg/cm^{2} ^{6}LiF had been evaporated. The Li-content of the target was determined after the measurements by dissolving the LiF in water. The Li-concentration of the solution was then obtained by flame emission spectroscopy in comparison with known standard solutions. We thus obtained the Li-content of the target independently of its chemical composition. The accuracy of that method is believed to be ± 3 %. The cross section at the calibration point ($E_{lab} = 2.6$ MeV, $\Theta_{cm} = 75^{o}$) is then given as $\frac{d\sigma}{d\Omega} = (143 \pm 4)$ mb/sr.

The angular distributions which have been normalized to that calibration point are shown in figs. 1 and 2. The solid lines are results of a phase shift analysis of the data.

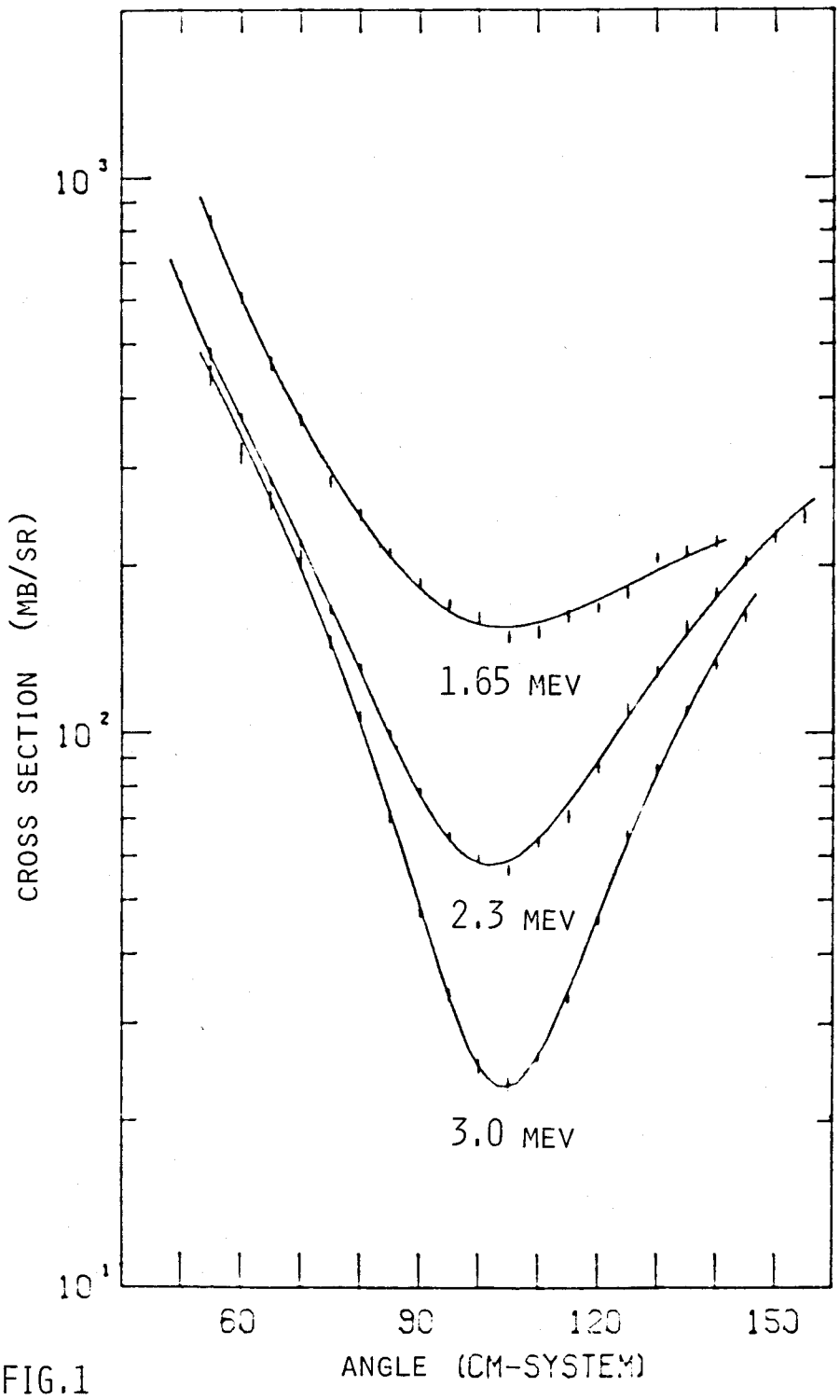

FIG.1

Angular distributions of α-particles scattered on ^{6}Li

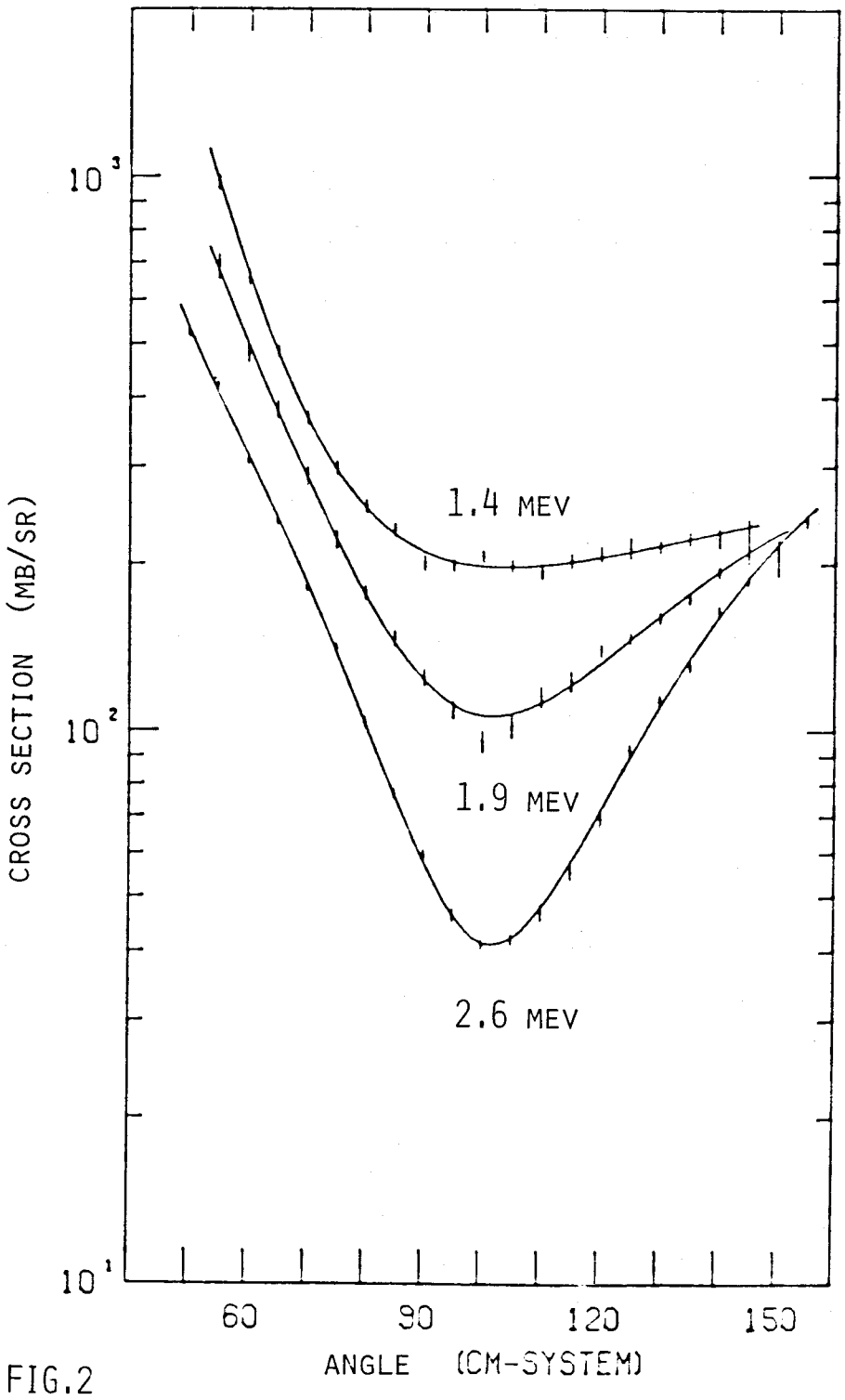

FIG.2

Angular distributions of α-particles scattered on ^{6}Li

IV. Eidg. Institut für Reaktorforschung (EIR), Würenlingen

(Dir.: Prof. Dr. H. Gränicher)

1. Measurement of the activation cross section of the reaction $^{93}Nb\ (n,n')\ ^{93m}Nb$ for 0 - 25 MeV neutrons

F. Hegedüs, M.W. Guinan†, J.R. Meadows†, N.F. Peek††
and L.R. Greenwood†††

The nobium is an excellent detector to monitor fast neutron fluence in power reactors {1,2,3,4}. However its use is quite limited because the cross section is not well known. At the Second ASTM - Euratom Symposium on Reactor Dosimetry (Palo Alto, October 1977) delegates from several countries have shown interest in a more accurate measurement of the cross section in the neutron energy range of 0-25 MeV. By that means it would be possible to extend generally the use of niobium detectors which could improve the accuracy of the present material damage dosimetry in power reactors. Furthermore the niobium could be used for material damage dosimetry in accelerator facilities and fusion devices, too.

The main problem with the cross section measurement is that the activation by means of discrete energy neutron sources is weak, because of the half life of the product is very long (11.4 y). On the other hand the thickness of the samples is limited (<10 mg/cm^2) because the energy of the counted X_k - rays is low (16.6 keV). Therefore only strong sources with continuous neutron spectra could be used to measure $\sigma(E)$.

The principle is that the niobium samples are activated along with a set of threshold detectors. This allows the determination of the neutron

† Lawrence Livermore Laboratory (LLL)
†† University of California, Davis (UCD)
††† Argonne National Laboratory (ANL)

spectra {5}, furthermore, by that means the unknown $\sigma(E)$ of niobium could be estimated by unfolding a number of integral experiments. Up to date only two measurements were published {1,4}, both used space dependent fast neutron spectra in fission reactors. The obtained accuracy was poor because the shape of their neutron spectra was not appropriate for this purpose: the differential neutron flux was too strongly decreasing with increasing neutron energy.

The neutron spectra of d-Be accelerator neutron sources have more suitable shapes for this purpose {6}. Specially the intense d-Be neutron source at the Crocker Nuclear Laboratory of the University of California at Davis {5} could be very appropriate to carry out the measurements of $\sigma(E)$ of niobium in the neutron energy range of 0-25 MeV.

Proposed Cross Section Evaluation

In 1977-78 a series of spectral determination experiments at d-Be sources were carried out at UC DAVIS, ANL & ORNL. In all these determinations the multiple foil techniques was used in which the $Nb^{93}(n,2n)Nb^{92m}$ reaction was included. The Nb foils are presently available and will be counted for Nb^{93m}. Five spectra at 30 MeV covering the angular range from 0-60°, two at 40 MeV (0° & 15°) and two at 15 MeV (0° & 15°) have been determined. In addition foils irradiated with D-T neutrons ($\hat{E} \sim 14.8$ MeV) at the RTNS facility at Lawrence Livermore Lab are available. Since the spectra differ substantially over the range from 1-25 MeV the Nb^{93m} cross section can be extracted from the integral measurements with reasonable precision.

References

{1} F. Hegedüs, Proceedings of the First ASTM-EURATOM Symposium on Reactor Dosimetry (Petten, 1975) 757

{2} R. Lloret, Proceedings (see ref. 1) 747

{3} F. Hegedüs, Proceedings of the Second ASTM-EURATOM Symposium on Reactor Dosimetry (Palo Alto, 1977) 825

{4} W.H. Taylor, Proceedings (see ref. 3) 831

{5} D.R. Nethaway, R.A. Van Konynenburg, M.W. Guinan and L.R. Greenwood, Proceedings of the Symposium on Neutron Cross Sections, Brookhaven 1977, BNL - NCS 50681, p. 135

{6} P.J. Persiani, W. Becker and J. Donahue, Proceedings (see ref. 5) 151

2. Radioisotope yields and cross sections in Lanthanum, Cesium and Iodine targets bombarded with 590 MeV protons

F. Hegedüs and N.F. Peek†

In 1976-77 a series of irradiations with 590 MeV protons at SIN were done with La_2O_3, $BaCO_3$, CsCl, NaI and NaBr targets to determine production yields of Xenon isotopes {1}. Later it was seen that the determination of other isotope yields from these experiments would be useful both for the medical isotope program of the EIR and for the radiation damage studies simulated by high energy protons (fusion program). The results of this study will be used in order to check the validity of the theoretical damage calculations {2}.

Three of the five target materials La_2O_3, CsCl and NaI were selected due to their close proximity in the chart of the nuclides. Furthermore, La, Cs and I are monoisotopic in their natural state.

In order to minimize the effects of secondary particles, relatively thin targets, irradiated alone (far away from other targets), were considered for evaluation.

The obtained cross sections as listed in Table 1 are classified in two ways: direct and cumulative. In general, direct cross sections of radioisotopes lying between two stable isobars were unambiguously determined.

† On leave from the University of California, Davis

Table 1. CROSS SECTION VS. Z AND A.

PRODUCT ISOTOPE			LANTHANUM TARGET									CESIUM TARGET					IODINE TARGET				
		HALF LIFE (H)				RUN A		RUN B		RUN C											
A*	Z		ΔZ	ΔA		σ (mb)	Δσ	σ (mb)	Δσ	σ (mb)	Δσ	ΔZ	ΔA		σ (mb)	Δσ	ΔZ	ΔA		σ (mb)	Δσ
-137	58	34.400	-1	2	DIR	4.43	1.80	3.21	1.10	3.00	1.00										
135	58	17.000	-1	4	DIR	5.72	.90	6.10	1.40	5.58	.60										
133	58	5.400	-1	6	DIR	1.78	.70	1.95	.70	1.95	.60										
132	58	4.200	-1	7	DIR	4.22	1.20	5.33	1.60	4.69	1.40										
130	58	.500	-1	9	DIR	2.10	.00	.70	.00	.50	.00										
135	57	19.500	0	4	CUM	25.40	7.00	33.30	10.00	28.10	8.50										
135	57	19.500	0	4	DIR	19.90	6.00	27.10	8.00	22.50	6.80										
132	57	4.500	0	7	CUM	17.30	5.00	20.80	6.00	19.50	5.00										
132	57	4.500	0	7	DIR	13.10	4.50	15.50	4.50	14.80	4.50										
131	57	1.020	0	8	CUM	19.30	2.00	20.90	6.00	18.50	3.70										
130	57	.145	0	9	DIR	6.00	.00	12.00	.00	8.00	.00										
-133	56	38.900	1	6	CUM	73.60	18.00	69.10	35.00	84.30	25.00										
131	56	276.000	1	8	CUM	39.90	5.00	50.60	10.00	43.70	4.50										
131	56	276.000	1	8	DIR	20.60	4.00	29.70	7.00	25.20	4.00	-1	2	DIR	7.80	.80					
-129	56	2.150	1	10	CUM	5.70	.00	7.30	.00	7.40	.00										
-129	56	2.150										-1	4	DIR	10.60	.00					
128	56	58.320	1	11	CUM	17.80	2.00	21.80	3.00	19.80	2.00										
128	56	58.320										-1	5	DIR	4.60	.90					
136	55	328.800	2	3	CUM	.96	.15	1.07	.32	1.06	.27										
132	55	158.160	2	7	CUM	7.86	.80	9.46	1.80	7.83	1.20										
132	55	158.160										0	1	DIR	77.50	8.00					
129	55	32.060	2	10	CUM	51.70	7.50	60.30	7.00	55.00	5.50	0	4	CUM	41.30	5.00					
129	55	32.060	2	10	DIR	46.00	6.50	53.00	8.50	47.60	9.50	0	4	DIR	31.20	6.00					
127	55	6.250	2	12	CUM	35.70	6.00	39.60	12.00	32.50	3.50	0	5	CUM	26.10	2.50					
125	55	.750	2	14	CUM	26.50	4.50	28.80	4.30	27.10	4.10	0	8	CUM	7.70	2.30					
127	54	873.740	3	12	CUM	61.70	5.50	67.90	10.00	65.50	6.60	1	5	CUM	69.50	7.00					
127	54	873.740	3	12	DIR	26.00	5.00	28.30	9.00	33.00	9.00										
125	54	17.200	3	14	CUM	41.90	7.00	50.40	8.00	45.10	6.00	1	8	CUM	50.30	5.00					
125	54	17.200	3	14	DIR	15.40	5.00	21.60	5.00	18.00	5.00	1	8	DIR	42.60	6.00	-1	2	DIR	3.70	.70
123	54	2.100	3	16	CUM	30.20	3.00	34.80	4.00	32.90	3.50	1	10	CUM	28.70	4.50					
123	54	2.100															-1	4	DIR	9.00	2.50
122	54	20.100	3	17	CUM	19.60	4.00	24.40	5.00	22.20	3.30	1	11	CUM	23.50	3.50					
122	54	20.100															-1	5	DIR	3.50	.70
121	54	.650	3	18	CUM	15.20	6.00	17.90	6.00	16.30	5.50	1	12	CUM	15.50	5.00					
120	54	.670	3	19	CUM	3.10	1.50	5.00	.00	5.00	.00	1	13	CUM	7.40	.00					

* - metastable state

Table 1. (cont.)

PRODUCT ISOTOPE			LANTHANUM TARGET									CESIUM TARGET					IODINE TARGET				
		HALF LIFE				RUN A		RUN B		RUN C											
A*	Z	(H)	ΔZ	ΔA		σ (mb)	Δσ	σ (mb)	Δσ	σ (mb)	Δσ	ΔZ	ΔA		σ (mb)	Δσ	ΔZ	ΔA		σ (mb)	Δσ
126	53	307.200	4	13	DIR	2.84	.60	3.00	.90	3.25	.65	2	7	DIR	11.20	1.60	0	1	DIR	64.50	6.50
124	53	100.080	4	15	DIR	6.56	.70	6.64	1.00	7.13	.70	2	9	DIR	17.20	1.70	0	3	DIR	30.60	3.10
123	53	13.300	4	16	CUM	43.50	9.00	50.90	10.00	49.80	9.00	2	10	CUM	63.70	10.50	0	4	CUM	42.20	6.50
123	53	13.300	4	16	DIR	13.20	7.00	16.10	8.00	16.90	8.00	2	10	DIR	35.00	7.00					
121	53	2.120	4	18	CUM	28.20	6.00	36.90	8.00	33.60	7.00	2	12	CUM	44.40	12.00	0	6	CUM	22.60	4.20
121	53	2.120	4	18	DIR	13.00	4.00	19.00	3.20	17.30	2.60	2	12	DIR	28.90	8.50					
120	53	1.350	4	19	CUM	14.00	5.00	17.70	5.00	18.00	5.00	2	13	CUM	28.50	5.00	0	7	CUM	13.90	4.00
120	53	1.350	4	19	DIR	10.90	5.00	.00	.00	.00	.00	2	13	DIR	21.10	4.00					
119	53	.320	4	20	CUM	14.70	3.00	16.00	3.50	18.40	3.50	2	14	CUM	18.80	.00	0	8	CUM	9.30	3.00
121	52	408.000	5	18	CUM	29.00	4.40	31.90	4.50	29.40	3.60	3	12	CUM	40.00	4.00	1	6	CUM	27.60	2.80
-121	52	3696.000	5	18	DIR	4.10	1.40	.00	.00	4.35	1.70	3	12	DIR	9.90	.00					
119	52	15.900	5	20	CUM	16.10	2.50	15.10	3.00	19.00	3.50	3	14	CUM	26.70	3.00	1	8	CUM	18.50	2.90
-119	52	112.320	5	20	DIR	7.80	1.20	9.30	1.50	8.40	1.10	3	14	DIR	17.60	3.50	1	8	DIR	20.40	4.00
118	52	144.000	5	21	CUM	10.00	1.70	14.60	3.50	10.80	1.60	3	15	CUM	15.50	5.00	1	9	CUM	42.20	19.00
117	52	1.083	5	22	CUM	15.60	1.40	18.40	2.50	15.80	2.10	3	16	CUM	27.60	5.00	1	10	CUM	19.90	2.50
116	52	2.500	5	23	CUM	11.60	3.00	13.20	3.00	14.40	3.00	3	17	CUM	21.00	4.00	1	11	CUM	15.00	2.70
122	51	64.800	6	17	DIR	.37	.11	.49	.12	.37	.09	4	11	DIR	12.20	3.50	2	5	DIR	5.10	.50
-120	51	139.200	6	19	DIR	1.18	.30	1.36	.30	1.26	.30	4	13	DIR	26.20	3.00	2	7	DIR	6.20	.60
-118	51	5.100	6	21	DIR	26.90	9.00	35.10	8.00	36.50	7.00	4	15	DIR	75.70	12.00	2	9	DIR	108.90	11.00
117	51	2.800	6	22	CUM	21.70	6.00	28.20	6.00	24.50	3.50	4	16	CUM	36.60	10.00	2	10	CUM	46.50	8.00
117	51	2.800	6	22	DIR	6.10	2.00	9.80	3.00	8.70	2.50	4	16	DIR	19.00	7.00	2	10	DIR	26.60	6.50
116	51	.250															2	11	DIR	6.20	2.50
115	51	.502	6	24	CUM	12.80	4.00	19.90	8.00	14.60	3.00	4	18	CUM	28.50	11.00	2	12	CUM	32.80	10.50
113	51	.115										4	20	CUM	7.30	.00					
-117	50	336.000	7	22	DIR	2.60	.00	2.90	.00	3.30	.00	5	16	DIR	10.40	.00					
113	50	2760.000	7	26	CUM	10.40	2.20	13.50	3.10	11.10	2.30	5	20	CUM	28.90	5.50					
110	50	4.000	7	29	CUM	.00	.00	.00	.00	2.50	.00	5	23	CUM	8.80	1.80	3	17	CUM	11.20	3.50
111	49	67.920	8	28	CUM	8.60	3.00	11.00	3.00	12.00	3.00	6	22	CUM	32.50	3.50	4	16	CUM	39.10	4.00
-110	49	4.900	8	29	DIR	2.60	.50	3.70	1.20	3.30	.60	6	23	DIR	8.50	.90	4	17	DIR	13.90	1.60
109	49	4.100	8	30	CUM	4.30	.00	5.30	.00	5.10	.00	6	24	CUM	14.20	3.50	4	18	CUM	22.10	5.40
108	49	.470	8	31	CUM	2.20	.00	2.20	.00	2.30	.00						4	19	CUM	10.10	4.00
115	48	53.500										7	14	DIR	.80	.30					

* - metastable state

Table 1. (cont.)

PRODUCT ISOTOPE			LANTHANUM TARGET									CESIUM TARGET					IODINE TARGET				
		HALF LIFE				RUN A		RUN B		RUN C											
A*	Z	(h)	ΔZ	ΔA		σ(mb)	Δσ	σ(mb)	Δσ	σ(mb)	Δσ	ΔZ	ΔA		σ(mb)	Δσ	ΔZ	ΔA		σ(mb)	Δσ
-106	47	204.000	10	33	DIR	1.16	.20	1.26	.20	1.12	.20	8	27	DIR	3.90	.50	6	21	DIR	7.90	1.20
105	47	960.000	10	34	CUM	2.69	.80	2.00	.00	2.60	.80	8	28	CUM	9.00	1.90	6	22	CUM	17.40	3.50
101	46	8.500										9	32	CUM	2.50	1.00	7	26	CUM	6.60	1.60
100	46	96.000	11	39	CUM	.20	.06	.27	.08	.25	.05	9	33	CUM	1.15	.20	7	27	CUM	3.50	.70
105	45	35.880	12	34	DIR	6.20	1.80	7.60	2.00	6.70	1.50	10	28	DIR	5.40	1.10	8	22	DIR	.30	.00
-101	45	103.200	12	38	DIR	.88	.30	1.03	.35	1.03	.20	10	32	DIR	1.60	.20	8	26	DIR	2.80	.80
100	45	70.800	12	39	DIR	.63	.25	.65	.30	.54	.25	10	33	DIR	2.15	.50	8	27	DIR	.50	.10
-99	45	4.700										10	34	CUM	1.40	.50	8	28	CUM	4.80	.90
99	45	336.400										10	34	DIR	.50	.00	8	28	DIR	1.50	.40
105	44	4.440															9	22	DIR	6.80	.00
103	44	950.400										11	30	DIR	.14	.00					
97	44	69.120										11	35	CUM	.13	.05	9	30	CUM	4.70	1.20
96	43	104.400										12	37	DIR	.74	.15	10	31	DIR	2.10	.40
95	43	20.000										12	38	CUM	.99	.20	10	32	CUM	3.10	.60
94	43	4.880										12	39	CUM	.49	.15	10	33	CUM	1.60	.30
-93	42	6.950										13	40	DIR	.30	.00	11	34	DIR	.95	.20
92	41	243.840															12	35	DIR	.12	.00
90	41	14.600															12	37	CUM	1.10	.30
89	40	78.400															13	38	CUM	1.20	.40
-87	39	14.000															14	40	CUM	.54	.00
87	39	30.000															14	40	CUM	.57	.00

* - metastable state

In the case of parent-daughter decay, the direct cross section of the daughter (σ_d) as well as the cumulative cross section of the parent (σ_p) was obtained by fitting the following function with the measured activity decay curve (A(t)):

$$A(t) = A_d(t = 0)\cdot \exp(-\lambda_d\cdot t) + A_p(t = 0)\,\frac{\lambda_d}{\lambda_d-\lambda_p}\,(\exp(-\lambda_p\cdot t)-\exp(-\lambda_d\cdot t))$$

where the obtained $A_d(t = 0)$ and $A_p(t = 0)$ activities are directly related to σ_d and σ_p respectively.

In many cases due to the short-lived parent activity, only cumulative cross sections could be calculated.

In this type of experiment it is highly probable that errors are propagated from many sources. Therefore, each isotope was considered separately. Besides the usual statistical and geometrical errors of counting, two more serious sources of errors occur. The first is due to the overlapping of gamma rays because the spallation process produces many radioisotopes. The second is due to the uncertainties of the absolute gamma decay intensities from little known decay schemes. The absolute intensities and half lives were taken from {3} and {4}.

Another source of error is that due to the secondary particle activation. This effect was minimized by using relatively thin targets irradiated far away from the other targets. The proton current, which was calculated from the induced ^{24}Na, ^{22}Na and ^{7}Be activities in Al foil shows an agreement on the three obtained current values within 3 %. This would mean the secondary particle current was small as compared to the primary 590 MeV proton current.

A wide range of spallation cross sections from 590 MeV protons were thus determined for La, Cs and I targets ($+1 > \Delta Z > -13$ and $-1 > \Delta A > -40$).

These cross section values should be compared to theoretical predictions. One such program for this purpose is the CROIX code developed at LASL {5}.

References

{1} N.F. Peek and F. Hegedüs, EIR Internal Report (submitted for publication to Int.J.Appl. Rad.Isot.)

{2} C.A. Coulter, D.M. Parkin and W.V. Green, J. Nucl. Mat. 67 (1977) 140

{3} Nuclear Data Sheets

{4} A. Ertmann and W. Soyka, Jul-1003-Ac, Vol. 1 (1974)

{5} D.G. Foster, Jr., Los Alamos Scientific Laboratory, private communication

V. Schweiz. Institut für Nuklearforschung (SIN), Villigen

(Dir.: Prof. Dr. J.P. Blaser)

Progress of plans for the spallation neutron source at SIN

W. Fischer

During the year 1978 the ideas on a spallation neutron source at SIN have been consolidated into an already fairly specified concept {1}. As a result of the symposium on applications of such neutron sources held at SIN we came to the conclusion that a continuous version exploits the capabilities of the SIN-accelerator system optimally. Furthermore, this mode would provide for the users in Europe a complementary neutron source to the planned pulsed SNS device at Rutherford Laboratory.

With the realization of the new SIN injector cyclotron we can expect a 600 MeV proton beam with a current of 1-2 mA. The continuous beam, after having passed the target stations for secondary pion and muon beams, would be refocused and sent to the heavy metal target of the continuous neutron station which would also act as a beam dump. The most attractive version of the target concepts investigated consists of a Pb/Bi-Eutecticum circulated by an electromagnetic pump through a heat exchanger, giving off the heat to a secondary circuit. The moderator assembly arranged around the target consists of an inner beryllium mantle and an external reflector of heavy water. Beryllium was chosen because of the possibility of neutron multiplication by (n,2n)-reactions of fast neutrons as well as due to technological reasons. The main advantage of heavy water is its low absorption cross section for thermal neutrons.

The yield in Pb/Bi is about 10 neutrons per incident proton - practically all of them by nuclear evaporation. Due to its low absorption cross section for neutrons a Pb/Bi target can, nevertheless, be a strong neutron source. With the arrangement, mentioned above, a thermal neutron flux of

3×10^{14} n/cm^2· sec may be obtained for a proton current of 2 mA. This corresponds to the flux in a so-called medium flux reactor. The epithermal part to be expected is higher than in a reactor, namely c. 1 % of the thermal flux. The losses by heat production are less than 1 MW due to the fact that the heat deposition on a Pb/Bi target amounts to only 40 MeV per neutron, a value which is five times lower compared to neutron production in a nuclear reactor. Moreover the γ-ray background is one order of magnitude smaller and the activation of the target material c. hundred times weaker than in a reactor of comparable neutron flux and no long-lived isotopes are produced. Thus the installation of a cold neutron source also becomes promising. If the lay-out of the neutron source is concentrated on the development of the cryogenic part of the moderator a flux of cold neutrons corresponding to that of the high flux reactor at Grenoble (institute Max von Laue-Paul Langevin) may be expected.

From the technical point of view the spallation neutron source at SIN could start working in 1984. Another valuable tool for the investigation of condensed matter with applications in physics, chemistry, material sciences and biology would then be available.

References

{1} W.E. Fischer, W. Joho, Ch. Tschalär, B. Sigg and H. Rauch, SIN Internal Report, December 1978

{2} W.E. Fischer, SIN Newsletter No. 11, March 1979, p. 8